Original Article

Performance Investigation of Marginalized Particle-Extended Kalman Filter under Different Particle Weighting Strategies in the Field of Electrocardiogram Denoising

Maryam Mohebbi, Hamed Danandeh Hesar

Department of Biomedical Engineering, K. N. Toosi University of Technology, Tehran, Iran

M. Mohebbi

ORCID ID

https://orcid.org/0000-0003-2326-6074

Abstract

Background: Recently, a marginalized particle-extended Kalman filter (MP-EKF) has been proposed for electrocardiogram (ECG) signal denoising. Similar to particle filters, the performance of MP-EKF relies heavily on the definition of proper particle weighting strategy. In this paper, we aim to investigate the performance of MP-EKF under different particle weighting strategies in both stationary and nonstationary noises. Some of these particle weighting strategies are introduced for the first time for ECG denoising. **Methods:** In this paper, the proposed particle weighting strategies use different mathematical functions to regulate the behaviors of particles based on noisy measurements and a synthetic ECG signal built using feature parameters of ECG dynamic model. One of these strategies is a fuzzy-based particle weighting method that is defined to adapt its function based on different input signal-to-noise ratios (SNRs). To evaluate the proposed particle weighting strategies, the denoising performance of MP-EKF was evaluated on MIT-BIH normal sinus rhythm database at 11 different input SNRs and in four different types of artificial and real noises. For quantitative comparison, the SNR improvement measure was used, and for qualitative comparison, the multi-scale entropy-based weighted distortion measure was used. **Results:** The experimental results revealed that the fuzzy-based particle weighting strategy exhibited a very well and reliable performance in both stationary and nonstationary noisy environments. **Conclusion:** We concluded that the fuzzy-based particle weighting strategy is the best-suited strategy for MP-EKF framework because it adaptively and automatically regulates the behaviors of particles in different noisy environments.

Keywords: *Electrocardiogram denoising, fuzzy logic, marginalized particle-extended Kalman filtering, model-based filtering, nonlinear Bayesian filtering*

Introduction

The electrocardiogram (ECG) signal is a noninvasive and powerful clinical tool to measure the cardiac activity and diagnose its related diseases. Although it is very easy to acquire, it is often corrupted by environmental and nonenvironmental interferences such as power line interference, bioelectric activities of the issues not belonging to the area of diagnostic interest, noise originating from electrode misplacement or other electrical instruments, electromyographic (EMG) noise or muscle artifact (MA), and ECG signal amplitude modulation with respiration.[1] Such unwanted interferences may change or corrupt the morphological properties of ECG beats which are crucial for correct cardiac analysis and diagnosis. Therefore, ECG denoising remains a major concern for researchers, and many methods have been proposed to address this issue. Adaptive filters are the most commonly used techniques applied to remove baseline wander, EMG, and MA noises from ECG signals.[2,3] Statistical approaches such as principal component analysis,[4] independent component analysis,[5,6] and neural networks[7] also have been proposed to suppress the effects of noise in ECG beats. Because ECG is a nonlinear nonstationary signal that possess multi-resolution properties, using wavelet transform has also been very popular in the

How to cite this article: Mohebbi M, Hesar HD. Performance investigation of marginalized particle-extended Kalman filter under different particle weighting strategies in the field of electrocardiogram denoising. J Med Sign Sens 2018;8:147-60.

Address for correspondence:
Dr. Maryam Mohebbi, Department of Biomedical Engineering, Electrical Faculty, K. N. Toosi University of Technology, P.O. Box 163151355, Tehran, Iran.
E-mail: m.mohebbi@kntu.ac.ir

Website: www.jmss.mui.ac.ir
DOI: 10.4103/jmss.JMSS_14_18

field of ECG denoising and processing.[8-12] More recently, techniques based on empirical mode decomposition[13-15] and variational mode decomposition[16] are also used to extract noise-free signal from noisy ECGs. Although there are a lot of nonmodel-based methods that can perform well in the field of ECG denoising, there are some undeniable benefits in using model-based approaches. As it is known, most physicians analyze ECG signals based on their morphologies and their diagnostic conclusions are mainly based on the shapes and morphological patterns of signals. For example, when a physician claims that an ECG record has premature ventricular contractions (PVCs), his/her deduction is based on the changes of morphological trends in normal ECG beats when PVCs happen. Model-based methods are computerized techniques that allow computers to analyze ECG records based on their morphologies, and thus, they can offer more benefits to physicians and clinical experts. However, model-based techniques need more calculation time which thanks to the advances in the development of powerful processors and parallel processing technologies; it is not a big deal anymore. In the field of model-based analysis of ECG, the ECG dynamic model (EDM) proposed by McSharry *et al*.[17] and its polar variants are very popular and have been used in model-based Bayesian filtering frameworks for ECG denoising, segmentation, and arrhythmia detection. Many of these Bayesian frameworks are based on extended Kalman filtering (EKF) approaches.[18-25] Since ECG has a nonlinear nature itself and some noises accompanying it (such as MA) are non-Gaussian and nonstationary, in some works, it was proposed to implement nonlinear Bayesian frameworks, i.e., particle filters (PFs) for ECG denoising.[26-29] In the study by Hesar and Mohebbi,[29] they proposed a marginalized particle-EKF (MP-EKF) that used marginalized particle filter (MPF) and EKF frameworks with a novel particle weighting strategy to denoise ECG signals efficiently. This framework was evaluated in both stationary and nonstationary environments and exhibited good performance over previous linear Bayesian frameworks, especially at low signal-to-noise ratios (SNRs) and in non-Gaussian environments. The MP-EKF in the study by Hesar and Mohebbi[29] benefitted from a particle weighting strategy which utilized synthetic ECG signals along with ECG signals to achieve better estimations. The synthetic ECG signals were built using EDM parameters and ECG linear phase wrapping.

The MP-EKF in the study by Hesar and Mohebbi[29] had some drawbacks:

1. Similar to other model-based methods, the MP-EKF in the study by Hesar and Mohebbi[29] could not perform well in ECG segments with varying morphologies or arrhythmia because its particle weighting strategy's trust level to measurements did not vary with respect to different morphologies
2. The parameters of EDM were not estimated properly using linear ECG phase wrapping, especially when angular frequency was changing significantly. This caused the synthetic ECG signal to be misaligned with respect to the original signal.

To address the first problem, an adaptive particle weighting strategy was proposed in the study by Hesar and Mohebbi[30] which enabled the MP-EKF to perform well in the presence of different arrhythmia and even in ECG lead disconnection situations. This strategy used fuzzy logic, correlation, and EDM feature parameters to adjust its trust level to handle different morphologies in a single ECG segment. To have better denoising outputs and maximal overlaps between synthetic ECG signals and their corresponding ECG signals, a nonlinear ECG phase wrapping based on dynamic time warping (DTW) was implemented which leads to better estimation of EDM parameters, more accurate synthetic ECG, and reliable particle weighting.[30] Unlike the first strategy proposed in the study by Hesar and Mohebbi[29] for MP-EKF, the behavior of fuzzy-based particle weighting strategy has not been investigated yet in different noisy environments. In this paper, first, we propose several new particle weighting strategies, and then, we evaluate the denoising performance of MP-EKF using different particle weighting strategies. To do so, the denoising performance of MP-EKF was evaluated on MIT-BIH normal sinus rhythm database at 11 different input SNRs and in four different types of artificial and real noises (Gaussian white noise, pink, brown, and real MA noise) for each particle weighting strategy. For quantitative comparison, the SNR improvement measure, and for qualitative comparison, the multi-scale entropy-based weighted distortion (MSEWPRD) measure were used. The results demonstrated that in comparison to previous strategies and the new nonlinear strategies proposed for MP-EKF in the field of ECG denoising, the fuzzy-based particle weighting strategy exhibited a very well and reliable performance in both stationary and nonstationary noisy environments from both SNR improvement and MSEWPRD viewpoints, especially at low-input SNRs.

This paper is organized as follows. Methods Section focuses on ECG phase wrapping, EDM extraction, MP-EKF theories, and equations. In Results Section, several new particle weighting strategies along with the fuzzy-based particle weighting strategy are presented. The experimental results and analyses are given in Discussion Section, and finally, conclusions are drawn in the last section.

Methods

In this section, first, the previous works for denoising ECG using MP-EKF are briefly reviewed. The first two subsections provide basic information for readers about EDM and MP-EKF theories and equations. It is worth to mention that some unwanted mathematical mistakes were present in the definition of MP-EKF in the studies by Hesar and Mohebbi[29,30] and they are corrected in

this paper. In the last subsection, we review the previous particle weighting strategies proposed for MP-EKF in the field of ECG denoising and introduce several other new strategies that are based on nonlinear mathematical operators that have the potential to be used inside MP-EKF framework.

The marginalized particle-extended Kalman filtering theory

In the study by Hesar and Mohebbi,[29] an MP-EKF-based filtering framework for ECG denoising was introduced. This framework used the polar variant of EDM that was proposed by Sameni *et al*.[18] The model in Eq. 1 describes the ECG signal as summation of several Gaussian Kernels corresponding to ECG feature segments, i.e., P, Q, R, S, and T waves in polar space. This model is given by:

$$\begin{cases} \varphi_{k+1} = \left(\varphi_k + \omega_k \delta\right) \bmod (2\pi) + \eta_\phi \\ z_{k+1} = -\sum_{j\in\{P,Q,R,S,T\}} \omega_k \delta \frac{a_j \Delta\theta_j}{b_j^2} \exp\left(-\frac{\Delta\theta_j^2}{2b_j^2}\right) + z_k + \eta \\ \omega_{k+1} = \omega_k + \eta_\omega \end{cases} \quad (1)$$

In the above model, φ_k, z_k, ω_k are phase, amplitude, and angular velocity at time-step k, respectively. In addition, $\Delta\theta_j = \left(\varphi_k - \theta_j\right) \bmod (2\pi)$, where δ is the sampling period, and the feature parameters a_j, b_j, θ_j $(j \in P, Q, R, S, T)$ are the amplitude, angular width, and location of each Gaussian Kernel, respectively. η_ϕ, η, and η_ω are random Gaussian white noises which model the uncertainty in EDM.

The measurement (observation) model in the study by Hesar and Mohebbi[29] was constructed using similar approaches in the studies by Sameni *et al*. and Sayadi *et al*.[18-20] In addition to noisy ECG amplitudes, two additional measurements were obtained. First R-peaks were detected, and linear phases (ranging from $-\pi$ to π) were assigned to ECG samples between each R-R interval. Another measurement was acquired by the differentiation of linear phase between two consecutive R-R peaks and considered as angular velocity observation. As a result, the measurement model is shown below:

$$\begin{bmatrix} \phi_k \\ s_k \\ \Omega_k \end{bmatrix} = \begin{bmatrix} 1 & 0 & 0 \\ 0 & 1 & 0 \\ 0 & 0 & 1 \end{bmatrix} . \begin{bmatrix} \varphi_k \\ z_k \\ \omega_k \end{bmatrix} + \begin{bmatrix} u_k \\ v_k \\ w_k \end{bmatrix}, \quad R_k = E\left\{ \left[u_k, v_k, w_k\right]^T \left[u_k, v_k, w_k\right] \right\} \quad (2)$$

where $y_k = [\phi_k, s_k, \Omega_k]^T$ is the measurement vector and the noise vector $v_k = [u_k, v_k, w_k]^T$ describes the measurement model's uncertainty. Eqs. 1 and 2 are rewritten into following form:

$$\mathrm{x}_{k+1}^{NL} = \mathrm{g}\left(\mathrm{x}_k^L, \omega_k^{NL}\right) + f_k^{NL}\left(\mathrm{x}_k^{NL}\right) \quad (3a)$$

$$\mathrm{x}_{k+1}^L = \left(A_k^L \mathrm{x}_k^L + G_k^L \omega_k^L\right) \bmod (2\pi) \quad (3b)$$

$$\mathrm{y}_k = h_k^{NL}\left(\mathrm{x}_k^{NL}\right) + C_k^L \mathrm{x}_k^L + \mathrm{e}_k \quad (3c)$$

In this model, $A_k^L = \begin{bmatrix} 1 & \delta \\ 0 & 1 \end{bmatrix}$,

$$\mathrm{x}_{k+1}^L = [\varphi_{k+1}, \omega_{k+1}]^T, \mathrm{x}_{k+1}^{NL} = z_{k+1}, f_k^{NL}\left(\mathrm{x}_k^{NL}\right) = z_k$$

$$\omega_k^{NL} = \left[\eta, a_j, b_j, \theta_j\right]^T \left(j \in P, Q, R, S, T\right), \omega_k^L = \left[\eta_\phi, \eta_\omega\right]^T$$

$$Q_k = \begin{pmatrix} Q_k^L & 0 \\ 0 & Q_k^{NL} \end{pmatrix}, Q_k^{NL} = E\{\omega_k^{NL}\left(\omega_k^{NL}\right)^T\}, Q_k^L = E\{\omega_k^L\left(\omega_k^L\right)^T\}$$

$$R_k = \begin{pmatrix} R_k^{NL} & 0 \\ 0 & R_k^L \end{pmatrix}, R_k^{NL} = E\{v_k v_k^T\}, R_k^L = E\{[u_k, w_k][u_k, w_k]^T\}$$

$$\mathrm{g}\left(\mathrm{x}_k^L, \omega_k^{NL}\right) = -\sum_{j\in\{P,Q,R,S,T\}} \omega_k \delta \frac{a_j \Delta\theta_j}{b_j^2} \exp\left(-\frac{\Delta\theta_j^2}{2b_j^2}\right) + \eta$$

In addition, $h_k^{NL}\left(\mathrm{x}_k^{NL}\right) = \begin{bmatrix} 0 \\ 1 \\ 0 \end{bmatrix} \mathrm{x}_k^{NL}$ and $C_k^L = \begin{bmatrix} 1 & 0 \\ 0 & 0 \\ 0 & 1 \end{bmatrix}$.

Considering the assumptions above, and inspired by MPF equations designed for mixed linear/nonlinear state models,[31] we proposed to implement an MP-EKF filtering framework for ECG denoising.[29] This method used a novel combination of marginalized particle filter and EKF frameworks to overcome the shortcomings of PF and EKF.

Eq. 3a is rewritten in the following form:

$$\xi_k = \mathrm{x}_{k+1}^{NL} - f_k^{NL}\left(\mathrm{x}_k^{NL}\right) = \mathrm{g}\left(\mathrm{x}_k^L, \omega_k^{NL}\right) \quad (4)$$

It can be deduced that although ξ_k is not an actual measurement of x_k^L, it has additional implicit information about x_k^L. Based on this idea and using EKF concept to linearly approximate $\mathrm{g}\left(\mathrm{x}_k^L, \omega_k^{NL}\right)$, the MP-EKF for ECG denoising is expressed in the following steps:

Step 1: For time-step $k=0$, with importance distribution $p_{\mathrm{x}_{0|0}^{NL}}(\mathrm{x}_{0|0}^{NL})$ and initialization mean $\overline{\mathrm{x}_0}$ and covariance matrix $\overline{P_0}$, initialize the particles $\mathrm{x}_{k|k}^{(i)} = \left[\mathrm{x}_{k|k}^{NL,(i)} \quad \mathrm{x}_{k|k}^{L,(i)}\right]^T$ for $i = 1, \ldots, N$, where $\mathrm{x}_{k|k}^{NL,(i)} \sim p_{\mathrm{x}_{0|0}^{NL}}(\mathrm{x}_{0|0}^{NL})$ and $\mathrm{x}_{k|k}^{L,(i)} \sim N(\bar{\mathrm{x}}_0, \bar{P}_0)$.

Step 2: calculate the importance weights $\left(w_k^{(i)}\right)$ for $i = 1, \ldots, N$ using $w_k^{(i)} = p\left(\mathrm{y}_k \mid X_k^{NL,(i)}, Y_{k-1}\right)$, where

$X_k^{NL,(i)} = \{x_{0|0}^{NL,(i)}, x_{1|1}^{NL,(i)}, \ldots, x_{k|k}^{NL,(i)}\}$, $x_{k|k}^{NL,(i)}$ is the nonlinear part of i^{th} estimated particle in time-step k and $Y_{k-1} = \{y_0, y_1, \ldots, y_{k-1}\}$, $x_{k|k}^{NL}$ is the nonlinear estimation of x_k^{NL} and it is a weighted summation of particles $x_{k|k}^{NL,(i)}$ $i = 1, \ldots, N$, i.e.,

$$x_{k|k}^{NL} = \sum_{i=1}^{N} w_k^{(i)} x_{k|k}^{NL,(i)} \tag{5}$$

Step 3: normalize importance weights:

$$\tilde{w}_k^{(i)} = \frac{w_k^{(i)}}{\sum_{j-1}^{N} w_k^{(j)}}$$

Step 4: If $\frac{1}{\sum_{j=1}^{N} (\tilde{w}_k^{(j)})^2} < N$, resample particles using systematic resampling.[32]

Step 5: For each particle $i = 1, \ldots, N$, perform Kalman filter measurement update according to:

$$\hat{x}_{k|k}^{L,(i)} = \hat{x}_{k|k-1}^{L,(i)} + K_k^{(i)} \left(y_k - h_k^{NL} \left(x_{k|k}^{NL,(i)} \right) - C_k^L \hat{x}_{k|k-1}^{L,(i)} \right) \tag{6a}$$

$$P_{k|k}^{(i)} = P_{k|k-1}^{(i)} - K_k^{(i)} C_k^L P_{k|k-1}^{(i)} \tag{6b}$$

$$S_k^{(i)} = C_k^L P_{k|k-1}^{(i)} (C_k^L)^T + R_k^L \tag{6c}$$

$$K_k^{(i)} = P_{k|k-1}^{(i)} (C_k^L)^T \left(S_k^{(i)} \right)^{-1} \tag{6d}$$

where $\hat{x}_{k|k}^{L,(i)}, P_{k|k}^{(i)}$, $K_k^{(i)}$, and $S_k^{(i)}$ are the estimated mean vector, covariance, Kalman gain, and measurement prediction covariance matrices for $x_k^{L,(i)}$ at time-step k, respectively.

Step 6: predict new particles for time-step $k+1$ using importance distribution according to Eq. 3, i.e.,

$$x_{k+1|k}^{NL,(i)} \sim p \left(x_{k+1|k}^{NL} \mid X_k^{NL,(i)}, Y_k \right) \tag{7}$$

Step 7: For each particle $i = 1, \ldots, N$, perform the first time update for the linear part of particle (first prediction) using:

$$\hat{x}_{k+1|k}^{L,(i),*} = A_k^L \hat{x}_{k|k}^{L,(i)} \tag{8a}$$

$$P_{k+1|k}^{(i),*} = A_k^L P_{k|k}^{(i)} \left(A_k^L \right)^T + Q_k^L \tag{8b}$$

where $\hat{x}_{k+1|k}^{L,(i),*}$ and $P_{k+1|k}^{(i),*}$ are the temporary representations of predicted mean vector and covariance matrix for the linear part of i^{th} particle at time-step $k + 1$, respectively.

Step 8: For each particle $i = 1, \ldots, N$, perform second Kalman filter prediction using:

$$\xi_k^{(i)} \approx g(\hat{x}_{k|k}^{L,(i)}, \bar{\omega}_k^{NL}) + \mathcal{A}_k \left(\hat{x}_{k+1|k}^{L,(i)} - \hat{x}_{k|k}^{L,(i)} \right) + \mathcal{B}_k \left(\omega_k^{NL} - \bar{\omega}_k^{NL} \right)$$

$$\mathcal{A}_k^{(i)} = \left(\frac{\partial g \left(\hat{x}_{k+1|k}^{L,(i)}, \bar{\omega}_k^{NL} \right)}{\partial \hat{x}_{k+1|k}^{L,(i)}} \Big| \hat{x}_{k+1|k}^{L,(i)} = \hat{x}_{k|k}^{L,(i)} \right)^T \tag{9a}$$

$$\mathcal{B}_k^{(i)} = \left(\frac{\partial g \left(\hat{x}_{k+1|k}^{L,(i)} \omega_k^{NL} \right)}{\partial \omega_k^{NL}} \Big| \omega_k^{NL} = \bar{\omega}_k^{NL} \right)^T$$

$$\hat{x}_{k+1|k}^{L,(i)} = \hat{x}_{k+1|k}^{L,(i),*} + L_k \left(\xi_k^{(i)} - g \left(\hat{x}_{k|k}^{L,(i)}, \bar{\omega}_k^{NL} \right) \right) \tag{9b}$$

$$P_{k+1|k}^{(i)} = P_{k+1|k}^{(i),*} - L_k^{(i)} N_k^{(i)} \left(L_k^{(i)} \right)^T \tag{9c}$$

$$L_k^{(i)} = A_k^L \left(x_k^{NL} \right) P_{k|k}^{(i)} (\mathcal{A}_k^{(i)})^T (N_k^{(i)})^{(-1)} \tag{9d}$$

$$N_k^{(i)} = \mathcal{A}_k^{(i)} P_{k|k}^{(i)} (\mathcal{A}_k^{(i)})^T + \mathcal{B}_k^{(i)} Q_k^{NL} (\mathcal{B}_k^{(i)})^T \tag{9e}$$

where $\hat{x}_{k+1|k}^{L,(i)}$ and $P_{k+1|k}^{(i)}$ are the predicted mean vector and covariance matrix for the linear part of particle $x_{k+1}^{(i)}$ at time-step $k + 1$, respectively.

Nonlinear electrocardiogram phase wrapping for electrocardiogram dynamic model extraction and synthetic electrocardiogram generation

The denoising performance of MP-EKF in the study by Hesar and Mohebbi[29] benefited from a synthetic signal called "ECG_{synth}" which had the same length as the original ECG signal and was built using the EDM characteristic parameters of that signal. Therefore, the construction of EDM is a very crucial step for MP-EKF as model-based framework. An accurate phase wrapping not only results in building a reliable EDM[33] but also leads to the construction of a more sensible synthetic ECG, which in turn improves the performance of the particle weighting strategy in MP-EKF. In prior studies, the parameters of EDM are estimated using linear polar ECG phase wrapping technique. However, linear phase wrapping is not accurate when angular frequency (ω_k) is changing significantly. This situation has two undesirable consequences: (1) The parameters of EDM are not estimated properly. (2) The synthetic ECG signal is misaligned with respect to the original signal. To solve this problem, in the study by Hesar and Mohebbi,[30] it was proposed to assign nonlinear phases to ECG samples using DTW approach proposed by Akhbari *et al*. and Niknazar *et al*.[25,34] To illustrate the differences between the linear and nonlinear phase wrapping approaches, two synthetic ECG signals are displayed in Figure 1. In Figure 1, although the angular frequency does not change

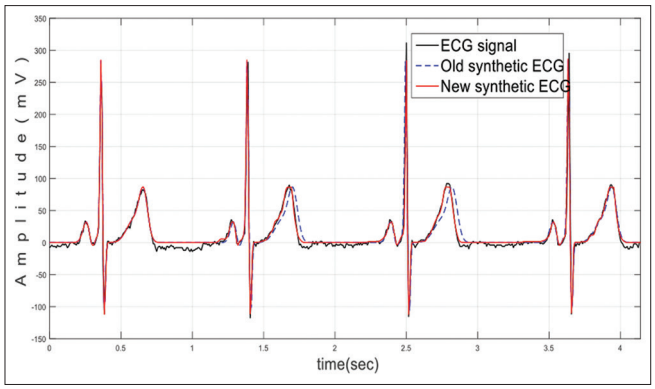

Figure 1: Comparison of synthetic electrocardiogram signals made with linear and nonlinear phase wrapping in an electrocardiogram segment from record "16272" (chosen from MIT-BIH normal sinus rhythm database[35])

considerably, it leads to an improper synthetic ECG formation. The synthetic signal made with linear phase wrapping approach in Figure 1 has some temporal delays that are visible on T waves (around 0.6 s and 2.7 s) with respect to ECG signal. These delays would impair the performance of MP-EKF in estimation of correct signal trajectories. However, the synthetic signal built based on nonlinear phase wrapping approach (new synthetic ECG) has an acceptable harmonic correspondence with ECG signal.

Theoretical aspects of different particle weighting strategies for marginalized particle-extended Kalman filtering in the field of electrocardiogram denoising

In the study by Hesar and Mohebbi,[29] it was suggested that to get better denoising results in noisy environments, the behaviors of particles in MP-EKF could be controlled based on the behaviors of both noisy and synthetic ECG signals. The particle weighting strategy in the study by Hesar and Mohebbi[29] used the following equation:

$$w_k^i = w_{k-1}^i \left(\frac{1}{d_{synth,k}^{(i)}} + \frac{1}{d_{measur,k}^{(i)}} \right) \tag{10}$$

where $d_{measur,k}^{(i)}$ is the Mahalanobis distance between the i^{th} particle at time-step k ($\left[\hat{\varphi}_{k|k}^{NL,(i)}\ \hat{z}_{k|k}^{NL,(i)}\ \hat{\omega}_{k|k}^{L,(i)}\right]^T$) and measurement vector at time-step k ($\left[\phi_k\ s_k\ \Omega_k\right]^T$) and $d_{synth,k}^{(i)}$ is the Mahalanobis distance between the i^{th} particle at time-step k and synthetic ECG signal at time-step k.[29]

The value of $d_{measur,k}^{(i)}$ characterizes the resemblance of the i^{th} particle to k^{th} noisy measurement. If $d_{measur,k}^{(i)}$ is small, it signifies that the i^{th} particle probably yields a good estimate of states and should get a higher weight and vice versa. The value of $d_{synth,k}^{(i)}$ characterizes the resemblance of the ith particle to the current sample in ECG_{synth}. If $d_{synth,k}^{(i)}$ is small, it implies that the i^{th} particle probably yields a good estimate of states and should get a higher weight and vice versa.

We can define other particle weighting strategies using nonlinear mathematical functions as well. For instance, the following equations use both $d_{synth,k}^{(i)}$ and $d_{measur,k}^{(i)}$ to regulate the performances of particles:

$$w_k^i = w_{k-1}^i \left(\frac{1}{d_{synth,k}^{(i)}} \times \frac{1}{d_{measur,k}^{(i)}} \right) \tag{11}$$

$$w_k^i = w_{k-1}^i \min\left(\frac{1}{d_{synth,k}^{(i)}}, \frac{1}{d_{measur,k}^{(i)}} \right) \tag{12}$$

$$w_k^i = w_{k-1}^i \max\left(\frac{1}{d_{synth,k}^{(i)}}, \frac{1}{d_{measur,k}^{(i)}} \right) \tag{13}$$

Each strategy in Eqs. 11–13 has specific properties. Eq. 12 imposes the strictest law to the particles. In Eq. 12, the weight of a single particle is high if and only if when that particle is very close to both synthetic and noisy ECG signals. This strategy is suitable for situations when the input SNR is low, and we want to suppress the noise effects. However, theoretically, at low-input SNRs, it does not guarantee a proper output. On the other hand, Eq. 13 has the most lenient rule. The weight of a particle in Eq. 13 is high when that particle is close to synthetic or noisy signal or both of them. Eq. 13 is appropriate for situations when the input SNR is high, and we want to trace the trajectory of ECG signal very accurately. However, at high-input SNRs, the particles are not supposed to trace the trajectories of signals exactly. Although the weighting strategy in Eq. 11 is stricter than Eq. 10, it is somewhat between rules of Eqs. 12 and 13. It is less lenient than Eq. 13 and less strict than Eq. 12. Theoretically, it can be used at mid-input SNRs. In the study by Hesar and Mohebbi,[30] it was proposed to use an adaptive particle weighting strategy that was derived from Eq. 10. As you know, Eq. 10 can be written as follows:

$$w_k^i = w_{k-1}^i \left(\frac{\alpha_1}{d_{synth,k}^{(i)}} + \frac{\alpha_2}{d_{measur,k}^{(i)}} \right) \tag{14}$$

where $\alpha_1 = \alpha_2 = 1$. However, hypothetically, α_1 can be different from α_2 if the power of noise is known. For example, for good signal tracing at high-input SNRs, α_2 can be set higher than α_1 (scenario 1). In very noisy signals, contrariwise, α_1 can be defined higher than α_2 (scenario 2). Therefore, Eq. 14 can be rewritten as the follows:

$$w_k^i = w_{k-1}^i \left(\frac{\alpha_1}{d_{synth,k}^{(i)}} + \frac{1-\alpha_1}{d_{measur,k}^{(i)}} \right) \quad (15)$$

One can see that while Eqs. 14 and 15 deliver similar results, Eq. 15 has fewer variables to deal with. For example in Eq. 15, at higher-input SNRs, α_1 can be tuned lower than 0.5 ($\alpha_1 < 0.5$ [scenario 1]), and at lower-input SNRs, it can be tuned higher than 0.5 ($\alpha_1 > 0.5$ [scenario 2]). In the study by Hesar and Mohebbi,[30] a fuzzy-based scheme was proposed that automatically and adaptively resolved these challenges. This scheme was based on two simple rules for ECG segments having normal beats. These rules are as follows:

- Rule 1: if λ_k is high, α_1 is low
- Rule 2: if λ_k is low, α_1 is high.

where

$$\lambda_k = \max(corr(ecg_{syn}(k-N+1:k), ecg_{noisy}(k-N+1:k))) \quad (16)$$

In Eq. 16, $corr(x,y)$ denotes the normalized cross-correlation function of two signals x and y and ecg_{syn} represents the synthetic signal (ECG_{synth}) and ecg_{noisy} denotes the real noisy ECG signal. As you can see, λ_k is the similarity factor in time-step k between noisy ECG signal and its synthetic representative.

Founded upon the aforementioned rules, a simple Sugeno-type fuzzy inference system was designed in the study by Hesar and Mohebbi.[30] Using fuzzy system, the particle weighting procedure in Eq. 15 is automatic and more adaptive. With this method, MP-EKF is able to automatically and adaptively balance its behavior with regard to different input SNRs.

For the rest of the paper, for simplification, let us denote the MP-EKFs using particle weighting strategies in Eqs. 10–15, "MP-EKF plus," "MP-EKF multiply," 'MP-EKF min," "MP-EKF max," and "MP-EKF fuzzy plus," respectively.

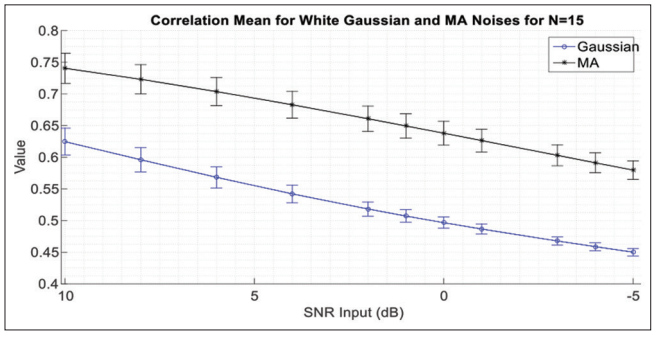

Figure 2: Mean and standard deviation of λ_k for DB1 in two noise types for n = 15 (muscle artifact and white Gaussian noise)[30]

Results

To investigate the proposed particle weighting strategies in the previous section, the performance of MP-EKF using each strategy was evaluated on MIT-BIH normal sinus rhythm database.[35] 200 signal segments from different subjects were selected from MIT-BIH normal sinus rhythm database (DB1). Each segment consisted of normal ECG beats with no significant arrhythmias with duration of 30 s and sampling frequency of 128 Hz. These segments were also used in the study by Hesar and Mohebbi[29] to evaluate the performance of MP-EKF over EKF/EKS frameworks. Four types of noise, Gaussian white noise, pink noise, brown noise, and MA noise, were selected for experiments. The first three noises were produced using the following spectral density:

$$S(f) \propto \frac{1}{f^{\beta}} \quad (17)$$

where $S(f)$ and f are the noise spectral density function and frequency in Hz. The parameter β is 0, 1, and 2 for Gaussian white, pink, and brown noise, correspondingly. For the nonstationary MA noise generation, real MA from the MIT-BIH Noise Stress Test Database was used.[36] This noise had a sampling rate of 360 Hz and it had to be resampled to 128 Hz (sampling frequency of test ECG segments). The SNRs 10, 8, 6, 4, 2, 1, 0, −1, −3, −4, −5 dB were chosen to simulate the same noisy situations in the study by Hesar and Mohebbi.[29] For quantitative comparison, the SNR improvement measure, and for qualitative comparison, the MSEWPRD[37] were used. The SNR improvement measure is given by:

$$\text{imp}[\text{dB}] = \text{SNR}_{\text{output}} - \text{SNR}_{\text{input}} = 10\log\left(\frac{\sum_i |x_n(i) - x_o(i)|^2}{\sum_i |x_d(i) - x_o(i)|^2} \right) \quad (18)$$

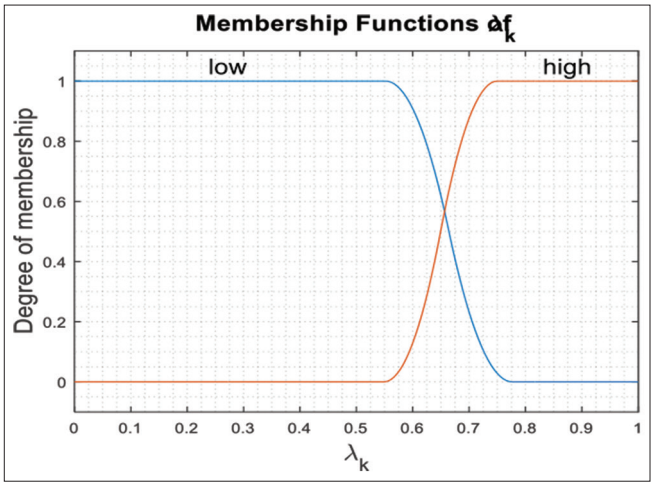

Figure 3: Fuzzy membership functions of λ_k[30]

where x_o, x_n, and x_d represent the original ECG signal, the noisy ECG signal, and the denoised ECG signal, respectively.[19] MSEWPRD is a weighted percentage root-mean-square difference (WPRD) between the subband wavelet coefficients of the original and filtered signals with weights equal to the multi-scale entropies of the corresponding subbands.[37] To calculate this metric, both signals must be decomposed using wavelet filters up to L levels. The number of levels depends on the nature of the signal and the sampling frequency. For sampling frequency of 128 Hz, we chose $L = 4$. The Daubechies 9/7 bi-orthogonal wavelet filters[38] were used for calculation of wavelet coefficients.

Before implementation of fuzzy-based particle weighting strategy in Eq. 15, to identify which values of λ_k, can be attributed as low or high, several experiments were conducted in the study by Hesar and Mohebbi.[30] For each segment in DB1, the values of λ_k were calculated and averaged in 11 input SNRs and for two noise types: the stationary white Gaussian noise and the nonstationary non-Gaussian MA noise. Figure 2 illustrates the mean and standard deviation of λ_k. It is realized that the values of λ_k for nonstationary MA noise are higher than those for stationary white Gaussian noise, which indicates that for an equal input SNR, α_1 can be set lower for MA noises. In other words, if the effect of nonlinear baseline drift is suppressed in noisy ECG, MP-EKF particles can trust noisy measurements more confidently.

Based on the results of Figure 2, the fuzzy membership functions of λ_k are constructed [Figure 3]. Next step is defining α_1. Many experiments were run to determine which values of α_1 would grant best results from SNR improvement and MSEWPRD viewpoints.[30] In these experiments, the range of "low α_1 " and "high α_1" were 0.3–0.49 and 0.51–0.6, respectively. Values outside these ranges were also examined but did not yield good MSEWPRD results. The experiments revealed that best results were achieved using values 0.48 and 0.52 for "low α_1" and "high α_1," respectively. The best results using these values are demonstrated in Figures 4-8.

In each SNR and in each simulation, each segment received a different random noise input. Similar to the study by Hesar and Mohebbi,[29] in this paper, the numbers of particles for all MP-EKFs were chosen 200 resulting 70–80 s calculation time for each simulation.

Figures 4 and 5 show the performance results of different MP-EKFs from SNR improvement viewpoint

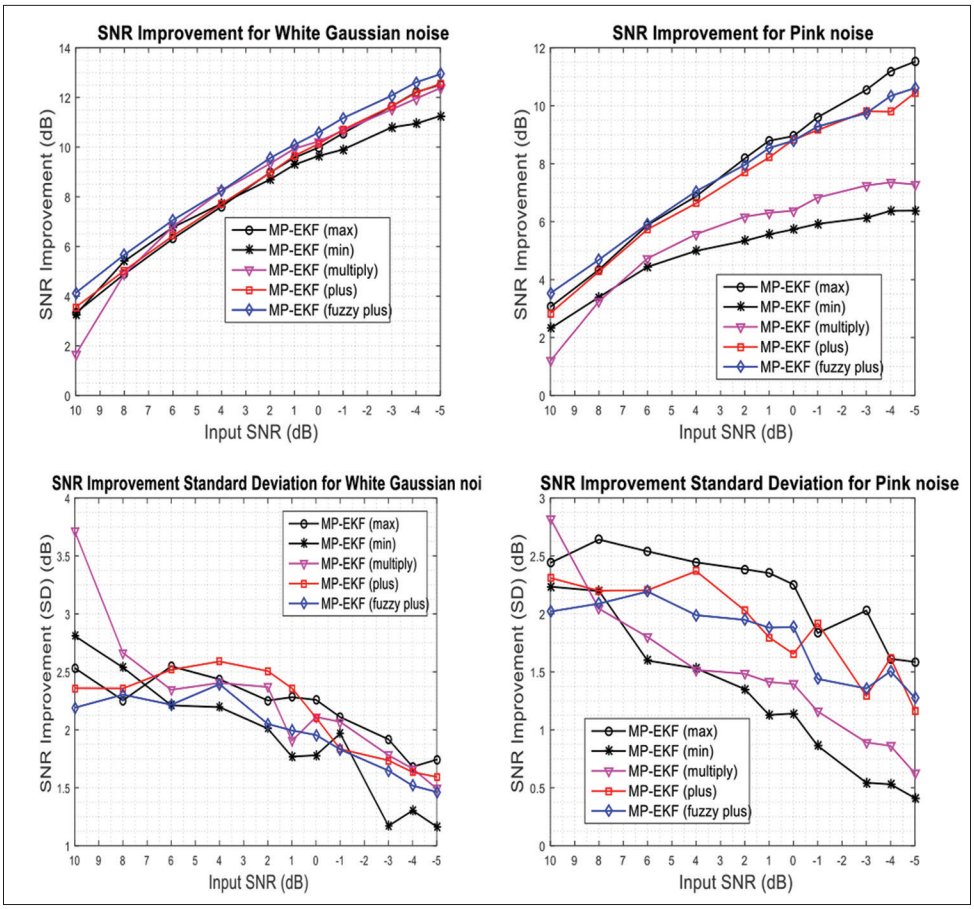

Figure 4: The mean (top) and standard deviation (bottom) of signal-to-noise ratio improvements versus different input signal-to-noise ratios for DB1 for marginalized particle-extended Kalman filter using different weighting strategies: (left) White Gaussian noise, (right) pink noise

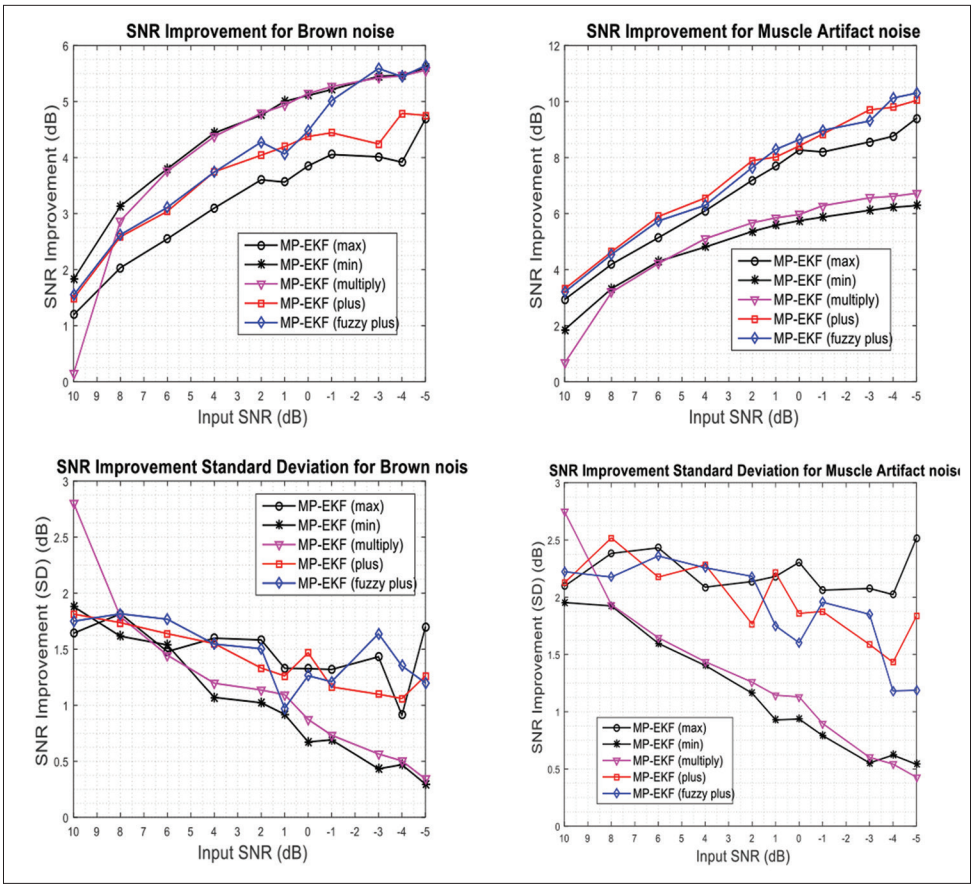

Figure 5: The mean (top) and standard deviation (bottom) of signal-to-noise ratio improvements versus different input signal-to-noise ratios for DB1 for marginalized particle-extended Kalman filter using different weighting strategies: (left) brown noise, (right) muscle artifact noise

in four noise types. It is clear in Figure 4 that "MP-EKF fuzzy plus" outperformed others in white Gaussian environments. At high-input SNRs and in white Gaussian noise, the performance of "MP-EKF min" was better than "MP-EKF plus," "MP-EKF max," and "MP-EKF multiply." However, at low-input SNRs, its performance was fallen below than others. "MP-EKF multiply" performed better than others in mid-SNRs, except "MP-EKF fuzzy plus." The performance of "MP-EKF max" was very similar (but not better) to "MP-EKF plus" for white Gaussian noise. Overall, it can be deduced that "MP-EKF fuzzy plus" and "MP-EKF plus" are appropriate choices for noisy environments corrupted by white Gaussian noise. For artificial pink and brown noises, the situation is different. In pink noises, although "MP-EKF fuzzy plus" proved to perform better than "MP-EKF plus," they were beaten by "MP-EKF max." Another fact that can be seen in Figure 4 is the low performance of both "MP-EKF multiply" and "MP-EKF min" for pink noises. Based on the results in Figure 4, "MP-EKF fuzzy plus" is a good choice for high-input and mid-input SNRs and "MP-EKF max" is a good choice for very low-input SNRs. Nevertheless, if we wanted a robust and stable performance for all input SNRs, "MP-EKF fuzzy plus" would be the proper option. By looking at Figure 5, it can be seen that for brown noise, "MP-EKF max" acted worst, and once again, "MP-EKF fuzzy plus" outmatched "MP-EKF plus." On the other hand, "MP-EKF multiply" and "MP-EKF min" performed better than others. However, at high-input SNRs, "MP-EKF multiply" could not achieve a desirable performance. The results in Figure 5 implied that it is recommended to use "MP-EKF min" for noisy environments corrupted by brown noise. In Figure 5, the performance results of the MP-EKFs for real MA noises are demonstrated. Like pink noise, "MP-EKF multiply" and "MP-EKF min" performed worse than others in MA noises. For MA noises, "MP-EKF fuzzy plus" achieved best results at low-input SNRs, and "MP-EKF plus" attained best results at high- and mid-input SNRs. From Figures 4 and 5, it can be concluded that from SNR improvement viewpoint, "MP-EKF fuzzy plus" yielded acceptable, reliable, and stable results in all types of noises and Eq. 15 can be attributed as the suitable particle weighting strategy for MP-EKF.

Discussion

In this paper, several particle weighting strategies are proposed in MP-EKF framework for ECG denoising. One

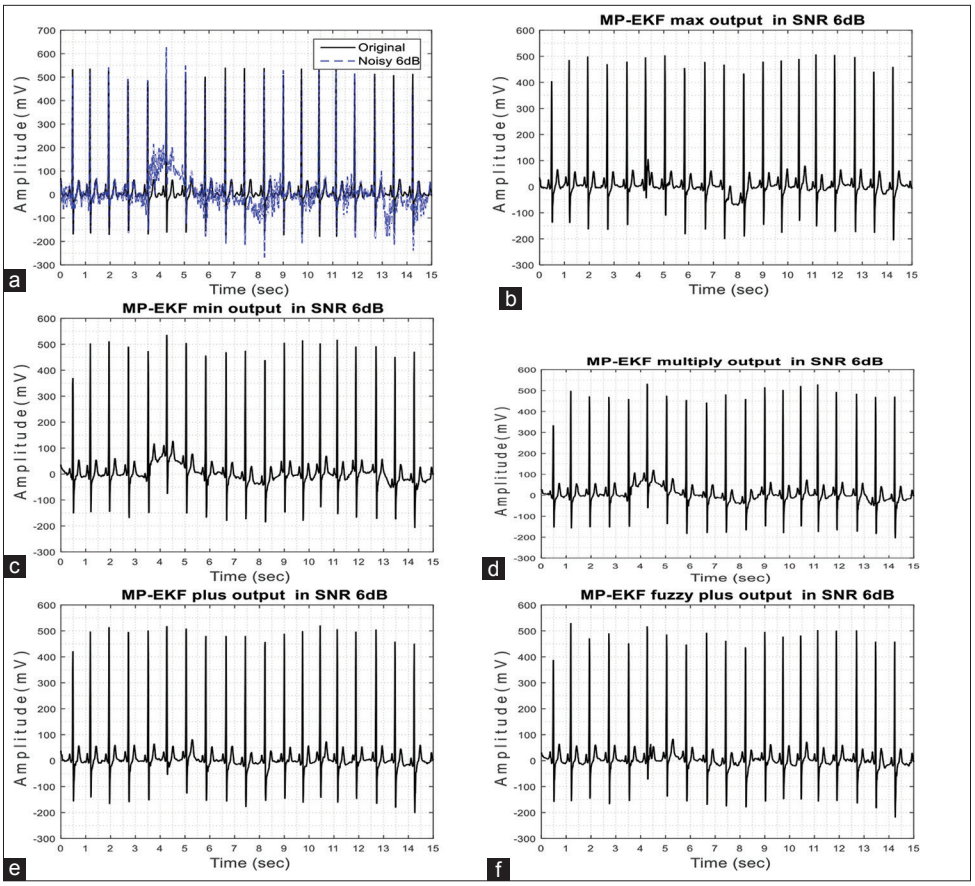

Figure 6: Typical filtering results for record "17453" from DB1 in the presence of muscle artifact noise in signal-to-noise ratio 6 dB. (a) Original and noisy, (b) "marginalized particle-extended Kalman filter max," (c) "marginalized particle-extended Kalman filter min," (d) "marginalized particle-extended Kalman filter multiply," (e) "marginalized particle-extended Kalman filter plus," (f) "marginalized particle-extended Kalman filter fuzzy plus"

of these strategies which proved to perform well in both Gaussian and non-Gaussian nonstationary environments was an adaptive fuzzy-based particle weighting strategy. This strategy manifested a noticeable superiority over other existing particle weighting strategies proposed for MP-EKF from SNR improvement viewpoint.

For further illustration, an example of denoising in the presence of MA noise is shown in Figure 6 to explore the behaviors of the proposed particle weighting strategies. It is mentioned earlier that "MP-EKF min" has the softest regulation on particles. It seems that this rule could not avoid particles in tracing the baseline drift. Another deficiency is seen around time interval 12.9–13.5 s when "MP-EKF min" failed to preserve the morphology of ECG. These shortcomings are somewhat present in the output of "MP-EKF multiply" [Figure 6d] too. However, "MP-EKF multiply" managed to suppress the baseline drift better than "MP-EKF min." The performance of "MP-EKF max" [Figure 6b] was better than the two aforementioned MP-EKFs. Although "MP-EKF max" could not recover the morphology of ECG completely in time interval 4.2–4.7 s, it removed the baseline drift effects in the most parts of ECG segment and preserved the morphology of ECG around time interval 12.9–13.5 s. From Figure 6e and f, it is inferred that "MP-EKF plus" and "MP-EKF fuzzy plus" are more successful than other MP-EKFs in dealing with MA noise. It is also realized that "MP-EKF plus" performed better than "MP-EKF fuzzy plus" in preserving the morphology of ECG. This fact can also be seen in the SNR improvement results for MA noises in Figure 5. As it is said earlier, the results in Figure 5 imply that for MA noises, at high- and mid-input SNRs, "MP-EKF plus" was superior to "MP-EKF fuzzy plus." However, at low-input SNRs, "MP-EKF fuzzy plus" outmatched "MP-EKF plus."

To explore the diagnostic distortion effects in the outputs of the aforementioned MP-EKFs, we calculated the MSEWPRD for DB1. The results are mentioned in Tables 1-4; however, for better view, they are illustrated in Figures 7 and 8. In Figure 7, it is clear that "MP-EKF fuzzy plus" attained the lowest MSEWPRD in white Gaussian noise at all input SNRs. This means that in white Gaussian interferences, "MP-EKF fuzzy plus" preserves the clinical information better than others. In pink noises, "MP-EKF max" along with "MP-EKF fuzzy plus" achieved lower MSEWPRDs. Although

Table 1: Performance evaluation of filtering frameworks for DB1 in the presence of white Gaussian noise from multi-scale entropy-based weighted distortion viewpoint

Method	MSEPWRD (mean±SD) (mV) Gaussian white noise										
	10 dB	8 dB	6 dB	4 dB	2 dB	1 dB	0 dB	−1 dB	−3 dB	−4 dB	−5 dB
MP-EKF fuzzy plus	0.248±0.065	0.259±0.074	0.276±0.070	0.304±0.087	0.326±0.073	0.351±0.084	0.367±0.071	0.386±0.081	0.434±0.081	0.472±0.098	0.505±0.090
MP-EKF max	0.268±0.081	0.276±0.072	0.303±0.095	0.327±0.096	0.347±0.091	0.365±0.095	0.393±0.101	0.410±0.093	0.451±0.099	0.480±0.088	0.548±0.141
MP-EKF min	0.278±0.097	0.269±0.088	0.287±0.0678	0.321±0.072	0.365±0.080	0.374±0.064	0.405±0.082	0.450±0.093	0.499±0.069	0.563±0.086	0.617±0.099
MP-EKF multiply	0.332±0.016	0.284±0.095	0.296±0.104	0.305±0.094	0.342±0.107	0.356±0.078	0.379±0.084	0.412±0.107	0.462±0.087	0.507±0.099	0.540±0.099
MP-EKF plus	0.254±0.073	0.277±0.084	0.294±0.090	0.316±0.090	0.355±0.111	0.377±0.117	0.380±0.083	0.404±0.085	0.475±0.105	0.493±0.103	0.538±0.120

MP-EKP – Marginalized particle-extended Kalman filter; SD – Standard deviation; MSEPWRD – Multi-scale entropy-based weighted distortion

Table 2: Performance evaluation of filtering frameworks for DB1 in the presence of pink noise from multi-scale entropy-based weighted distortion viewpoint

Method	MSEPWRD (mean±SD) (mV) Pink noise										
	10 dB	8 dB	6 dB	4 dB	2 dB	1 dB	0 dB	−1 dB	−3 dB	−4 dB	−5 dB
MP-EKF fuzzy plus	0.268±0.066	0.292±0.074	0.325±0.081	0.345±0.079	0.402±0.098	0.414±0.085	0.455±0.098	0.475±0.082	0.574±0.121	0.609±0.111	0.648±0.116
MP-EKF max	0.282±0.081	0.306±0.097	0.315±0.082	0.363±0.114	0.381±0.110	0.406±0.114	0.453±0.146	0.466±0.106	0.521±0.119	0.577±0.128	0.588±0.094
MP-EKF min	0.304±0.091	0.334±0.097	0.356±0.069	0.416±0.090	0.499±0.083	0.516±0.085	0.580±0.096	0.625±0.082	0.745±0.110	0.807±0.115	0.886±0.140
MP-EKF multiply	0.344±0.124	0.332±0.075	0.357±0.091	0.406±0.088	0.452±0.091	0.498±0.092	0.540±0.094	0.571±0.101	0.695±0.107	0.738±0.100	0.830±0.134
MP-EKF plus	0.296±0.087	0.302±0.081	0.317±0.076	0.370±0.100	0.411±0.093	0.438±0.095	0.433±0.070	0.497±0.103	0.556±0.076	0.649±0.147	0.638±0.099

MP-EKP – Marginalized particle-extended Kalman filter; SD – Standard deviation; MSEPWRD – Multi-scale entropy-based weighted distortion

Table 3: Performance evaluation of filtering frameworks for DB1 in the presence of brown noise from multi-scale entropy-based weighted distortion viewpoint

Method	MSEPWRD (mean±SD) (mV)										
	Brown noise										
	10 dB	8 dB	6 dB	4 dB	2 dB	1 dB	0 dB	−1 dB	−3 dB	−4 dB	−5 dB
MP-EKF fuzzy plus	0323±0.075	0.362±0.088	0.410±0.098	0.468±0.110	0.531±0.092	0.606±0.112	0.637±0.149	0.698±0.171	0.763±0.245	0.865±0.233	0.956±0.194
MP-EKF max	0.339±0.073	0.372±0.096	0.436±0.103	0.495±0.126	0.579±0.141	0.623±0.092	0.707±0.177	0.771±0.153	0.892±0.208	1.100±0.277	1.107±0.296
MP-EKF min	0.314±0.072	0.324±0.082	0.373±0.084	0.408±0.102	0.493±0.104	0.524±0.099	0.572±0.108	0.640±0.0113	0.724±0.140	0.808±0.157	0.926±0.153
MP-EKF multiply	0.354±0.133	0.339±0.088	0.357±0.072	0.421±0.080	0.500±0.101	0.532±0.084	0.581±0.102	0.632±0.124	0.768±0.113	0.790±0.180	0.920±0.174
MP-EKF plus	0.323±0.069	0.376±0.095	0.408±0.100	0.480±0.122	0.561±0.087	0.613±0.140	0.656±0.0125	0.694±0.120	0.966±0.232	1.027±0.258	1.067±0.251

MP-EKP – Marginalized particle-extended Kalman filter; SD – Standard deviation; MSEPWRD – Multi-scale entropy-based weighted distortion

Table 4: Performance evaluation of filtering frameworks for DB1 in the presence of muscle artifact noise from multi-scale entropy-based weighted distortion viewpoint

Method	MSEPWRD (mean±SD) (mV)										
	MA noise										
	10 dB	8 dB	6 dB	4 dB	2 dB	1 dB	0 dB	−1 dB	−3 dB	−4 dB	−5 dB
MP-EKF fuzzy plus	0.281±0.072	0.308±0.078	0.338±0.090	0.399±0.095	0.438±0.127	0.447±0.080	0.478±0.088	0.522±0.146	0.623±0.162	0.636±0.125	0.684±0.146
MP-EKF max	0.290±0.071	0.320±0.087	0.360±0.094	0.404±0.089	0.445±0.094	0.467±0.098	0.495±0.112	0.558±0.123	0.666±0.157	0.719±0.172	0.752±0.226
MP-EKF min	0.339±0.087	0.336±0.092	0.401±0.077	0.468±0.091	0.545±0.099	0.594±0.098	0.643±0.098	0.706±0.114	0.850±0.142	0.940±0.158	1.037±0.166
MP-EKF multiply	0.398±0.128	0.380±0.095	0.417±0.093	0.459±0.081	0.527±0.087	0.580±0.099	0.640±0.110	0.680±0.105	0.810±0.121	0.898±0.142	0.990±0.162
MP-EKF plus	0.279±0.072	0.301±0.084	0.320±0.078	0.392±0.105	0.416±0.094	0.465±0.124	0.498±0.117	0.530±0.126	0.587±0.127	0.631±0.126	0.727±0.223

MP-EKP – Marginalized particle-extended Kalman filter; SD – Standard deviation; MA – Muscle artifact; MSEPWRD – Multi-scale entropy-based weighted distortion

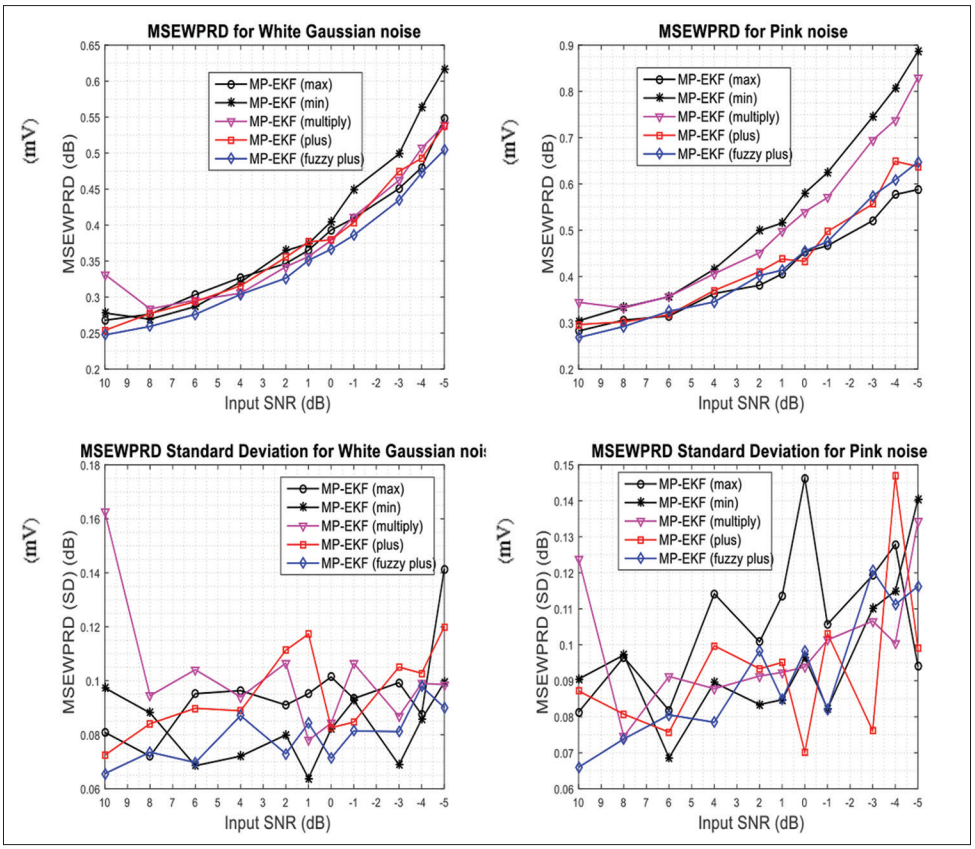

Figure 7: The mean (top) and standard deviation (bottom) of multi-scale entropy-based weighted distortions versus different input signal-to-noise ratios for DB1 for marginalized particle-extended Kalman filter using different weighting strategies: (left) white Gaussian noise, (right) pink noise

"MP-EKF fuzzy multiply" and "MP-EKF min" did not yield desirable results for white Gaussian, pink, and MA noises, they surprisingly managed to outperform other methods in brown noises [Figure 8]. In MA noises, as it is shown in Figure 8, "MP-EKF fuzzy plus" and "MP-EKF plus" performed better than others. At high- and mid-input SNRs, "MP-EKF plus" was better than "MP-EKF fuzzy plus;" however, at low-input SNRs, "MP-EKF fuzzy plus" was superior. Based on the SNR improvement and MSEWPRD results in Figures 4, 5, 7, 8, and Tables 1-4, we concluded that in comparison to other proposed strategies for MP-EKF in the field of ECG denoising, the fuzzy-based adaptive particle weighting strategy is still the best-suited strategy for MP-EKF framework.

Conclusion

In this paper, we explored the performance of MP-EKF under different particle weighting strategies in both stationary and nonstationary noises. In this paper, we proposed three novel nonlinear particle strategies that unlike adaptive fuzzy-based strategy, these new strategies did not need any preprocessing or knowledge about ECG segments which make them easy to implement. Despite introducing new particle weighting strategies in this paper, the experimental results revealed that the fuzzy-based particle weighting adaptive fuzzy-based strategy demonstrated better performance in many input SNRs and was more reliable than others in most types of noises, although in certain types of noises (e.g., brown noise), the dominance of adaptive fuzzy-based strategy was broken by one of the newly proposed particle weighting strategies. With adaptive fuzzy-based strategy, the MP-EKF can adaptively adjust its behavior with respect to different input SNRs and nonstationary environments. This particle weighting strategy automatically controls the behavior of particles according to input SNRs. At low-input SNRs, this strategy lowers the particles' degree of trust to the measurements while increasing their degree of trust to the synthetic ECG. At high-input SNRs, the particles' degree of trust to the measurements is increased and the degree of trust to synthetic ECG is decreased. To further improve the performance of MP-EKF, we used nonlinear phase wrapping in its observation model using DTW.

Financial support and sponsorship

None.

Conflicts of interest

There are no conflicts of interest.

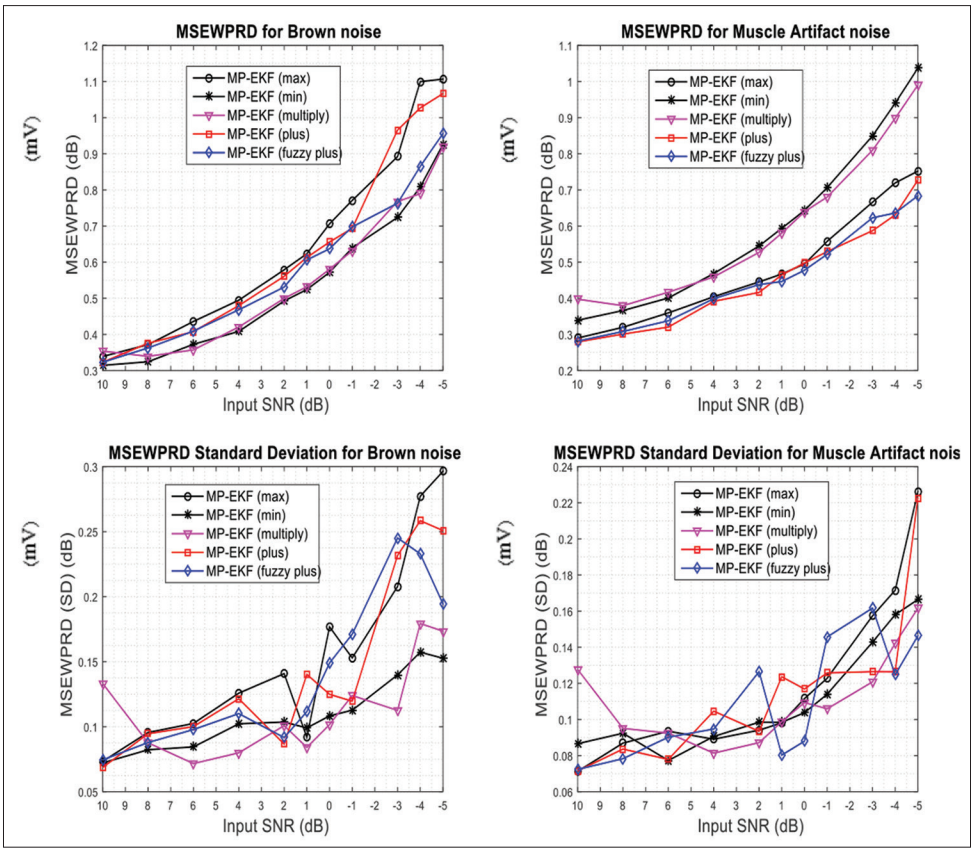

Figure 8: The mean (top) and standard deviation (bottom) of multi-scale entropy-based weighted distortions versus different input signal-to-noise ratios for DB1 for marginalized particle-extended Kalman filter using different weighting strategies: (left) brown noise, (right) muscle artifact noise

References

1. Friesen GM, Jannett TC, Jadallah MA, Yates SL, Quint SR, Nagle HT, *et al*. A comparison of the noise sensitivity of nine QRS detection algorithms. IEEE Trans Biomed Eng 1990;37:85-98.
2. Laguna P, Jané R, Meste O, Poon PW, Caminal P, Rix H, *et al*. Adaptive filter for event-related bioelectric signals using an impulse correlated reference input: Comparison with signal averaging techniques. IEEE Trans Biomed Eng 1992;39:1032-44.
3. Thakor NV, Zhu YS. Applications of adaptive filtering to ECG analysis: Noise cancellation and arrhythmia detection. IEEE Trans Biomed Eng 1991;38:785-94.
4. Moody GB, Mark RG, editors. QRS morphology representation and noise estimation using the Karhunen-Loeve transform. Computers in Cardiology. Jerusalem, Israel: IEEE; 1989.
5. Barros AK, Mansour A, Ohnishi N. Removing artifacts from electrocardiographic signals using independent components analysis. Neurocomputing 1998;22:173-86.
6. He T, Clifford G, Tarassenko L. Application of independent component analysis in removing artefacts from the electrocardiogram. Neural Comput Appl 2006;15:105-16.
7. Clifford G, Tarassenko L, Townsend N. One-pass training of optimal architecture auto-associative neural network for detecting ectopic beats. Electron Lett 2001;37:1126-7.
8. Donoho DL. De-noising by soft-thresholding. IEEE Trans Inf Theory 1995;41:613-27.
9. Kestler H, Haschka M, Kratz W, Schwenker F, Palm G, Hombach V, *et al*., editors. De-noising of high-resolution ECG signals by combining the discrete wavelet transform with the Wiener filter. Computers in Cardiology. Cleveland, OH, USA: IEEE; 1998.
10. Agante P, De Sá JM, editors. ECG noise filtering using wavelets with soft-thresholding methods. Computers in Cardiology. Hannover, Germany: IEEE; 1999.
11. Popescu M, Cristea P, Bezerianos A, editors. High resolution ECG filtering using adaptive Bayesian wavelet shrinkage. Computers in Cardiology. Cleveland, OH, USA: IEEE; 1998.
12. Sayadi O, Shamsollahi MB. Multiadaptive bionic wavelet transform: Application to ECG denoising and baseline wandering reduction. EURASIP J Adv Signal Process 2007;2007:1-11.
13. Chacko A, Ari S, editors. Denoising of ECG signals using Empirical Mode Decomposition Based Technique. International Conference on Advances in Engineering, Science and Management (ICAESM). Nagapattinam, Tamil Nadu, India: IEEE; 2012.
14. Mijović B, De Vos M, Gligorijević I, Taelman J, Van Huffel S. Source separation from single-channel recordings by combining empirical-mode decomposition and independent component analysis. IEEE Trans Biomed Eng 2010;57:2188-96.
15. Samadi S, Shamsollahi MB, editors. ECG noise reduction using empirical mode decomposition based on combination of instantaneous half period and soft-thresholding. 2nd Middle East Conference on Biomedical Engineering. Doha, Qatar: IEEE; 2014.
16. Lahmiri S. Comparative study of ECG signal denoising by wavelet thresholding in empirical and variational mode decomposition domains. Healthc Technol Lett 2014;1:104-9.
17. McSharry PE, Clifford GD, Tarassenko L, Smith LA.

A dynamical model for generating synthetic electrocardiogram signals. IEEE Trans Biomed Eng 2003;50:289-94.
18. Sameni R, Shamsollahi MB, Jutten C, Clifford GD. A nonlinear Bayesian filtering framework for ECG denoising. IEEE Trans Biomed Eng 2007;54:2172-85.
19. Sayadi O, Shamsollahi MB. ECG denoising and compression using a modified extended Kalman filter structure. IEEE Trans Biomed Eng 2008;55:2240-8.
20. Sayadi O, Shamsollahi MB. A model-based Bayesian framework for ECG beat segmentation. Physiol Meas 2009;30:335-52.
21. Sayadi O, Shamsollahi MB, Clifford GD. Robust detection of premature ventricular contractions using a wave-based bayesian framework. IEEE Trans Biomed Eng 2010;57:353-62.
22. Akhbari M, Shamsollahi MB, Jutten C, Coppa B, editors. ECG denoising using angular velocity as a state and an observation in an extended Kalman filter framework. EMBC; 2012: IEEE.
23. Montazeri Ghahjaverestan N, Shamsollahi MB, Ge D, Hernández AI. Switching Kalman filter based methods for apnea bradycardia detection from ECG signals. Physiol Meas 2015;36:1763-83.
24. Oster J, Behar J, Sayadi O, Nemati S, Johnson AE, Clifford GD, *et al*. Semisupervised ECG ventricular beat classification with novelty detection based on switching Kalman filters. IEEE Trans Biomed Eng 2015;62:2125-34.
25. Akhbari M, Shamsollahi MB, Jutten C, Armoundas AA, Sayadi O. ECG denoising and fiducial point extraction using an extended Kalman filtering framework with linear and nonlinear phase observations. Physiol Meas 2016;37:203-26.
26. Lin C, Bugallo M, Mailhes C, Tourneret JY, editors. ECG Denoising Using a Dynamical Model and a Marginalized Particle Filter. Asilomar Conference on Recombinant. Pacific Grove, CA: IEEE; 2011.
27. Lee J, McManus DD, Bourrell P, Sörnmo L, Chon KH. Atrial flutter and atrial tachycardia detection using Bayesian approach with high resolution time–frequency spectrum from ECG recordings. Biomed Signal Process Control 2013;8:992-9.
28. Hesar HD, Mohebbi M, editors. Muscle artifact cancellation in ECG signal using a dynamical model and particle filter. 22nd Iranian Conference on Biomedical Engineering (ICBME). Tehran, Iran: IEEE; 2015.
29. Hesar HD, Mohebbi M. ECG denoising using marginalized particle extended Kalman filter with an automatic particle weighting strategy. IEEE J Biomed Health Inform 2017;21:635-44.
30. Hesar HD, Mohebbi M. An adaptive particle weighting strategy for ECG denoising using marginalized particle extended Kalman filter: An evaluation in arrhythmia contexts. IEEE J Biomed Health Inform 2017;21:1581-92.
31. Schon T, Gustafsson F, Nordlund PJ. Marginalized particle filters for mixed linear/nonlinear state-space models. IEEE Trans Signal Process 2005;53:2279-89.
32. Martino L, Elvira V, Louzada F. Effective sample size for importance sampling based on discrepancy measures. Signal Process 2017;131:386-401.
33. Clifford G, Shoeb A, McSharry P, Janz B. Model-based filtering, compression and classification of the ECG. Int J Bioelectromagn 2005;7:158-61.
34. Niknazar M, Rivet B, Jutten C, editors. Application of dynamic time warping on Kalman filtering framework for abnormal ECG filtering. European Symposium on Artificial Neural Networks, Computational Intelligence and Machine Learning. ESANN: Bruges, Belgium; 2012.
35. The MIT-BIH Normal Sinus Rhythm Database. PhysioNet, Cambridge, MA. Available from: http://www.physionet.org/physiobank/database/nsrdb/. [Last accessed on 2018 June 18].
36. The MT-BIH Noise Stress Test Database. PhysioNet, Cambridge, MA. Available from: https://www.physionet.org/physiobank/database/nstdb/. [Last accessed on 2018 June 18].
37. Manikandan MS, Dandapat S. Multiscale entropy-based weighted distortion measure for ECG coding. IEEE Signal Process Lett 2008;15:829-32.
38. Antonini M, Barlaud M, Mathieu P, Daubechies I. Image coding using wavelet transform. IEEE Trans Image Process 1992;1:205-20.

BIOGRAPHIES

Maryam Mohebbi was born in Tehran, Iran, in 1981. She received the Ph.D. degree in biomedical engineering, from Tarbiat Modares University, in 2011. Currently, she is an Assistant Professor with the Department of Electrical Engineering, K. N. Toosi University of Technology, Tehran, Iran. Her research interests include biomedical signal processing, nonlinear analysis of HRV and ECG signals, model-based ECG processing, as well as EEG signal analysis and computational neuroscience.

Email: m.mohebbi@kntu.ac.ir

Hamed Danandeh Hesar was born in Urmia, Iran, in 1986. He received his B.Sc. degree in bioelectrical engineering from Sahand University of Technology, Iran in 2009 and the M.Sc. degree in bioelectrical engineering from K. N. Toosi University of Technology, Tehran, Iran in 2011. He obtained his Ph.D. degree in bioelectrical engineering from K. N. Toosi University of Technology in Feb, 2018. His research interests include statistical medical signal processing, ballistic image processing and multi-target tracking in microscopic videos.

Email: h_danandeh@ee.kntu.ac.ir